Contribution to International Workshop [1] on Hadron Structure and Hadron Spectroscopy,
Trieste, Italy, Feb. 2002

Pion Polarizabilities at CERN COMPASS

MURRAY MOINESTER [1]
FOR THE COMPASS COLLABORATION
R. and B. Sackler Faculty of Exact Sciences,
School of Physics and Astronomy, Tel Aviv University,
69978 Tel Aviv, Israel
murraym@tauphy.tau.ac.il

Abstract:

Objective:

The electric ($\bar{\alpha}$) and magnetic ($\bar{\beta}$) pion Compton polarizabilities characterize the pion's deformation in the electromagnetic field of the γ during $\gamma\pi$ Compton scattering. They depend on the rigidity of the pion's internal structure as a composite particle. The polarizabilities deduced by Antipov et al. in their low statistics Primakoff experiment ($\sim$ 7000 events) were $\bar{\alpha}_\pi = -\bar{\beta}_\pi = 6.8 \pm 1.4 \pm 1.2$, in units of 10^{-43} cm^3. This value, ignoring the large error bars, is about three times larger than the chiral perturbation theory (χPT) prediction. Taking into account the very high beam intensity, fast data acquisition, high acceptance and good resolution of the CERN COMPASS experiment, one can expect from COMPASS statistics a factor 6000 higher, a data sample that includes many tests to control systematic errors, and a significantly reduced total measurement uncertainty for $\bar{\alpha}_\pi$, of order 0.4.

Methodology:

CERN COMPASS studies pion-photon interactions to achieve a unique Primakoff physics program centered on pion polarizability studies. We will use a 190 GeV pion beam and a virtual photon target, and magnetic spectrometers and calorimeters to measure the complete kinematics of pion-photon reactions. COMPASS was set up during 2000/01, including a successful Primakoff test run, and then began data taking with a muon beam for the proton spin physics component of its program. COMPASS will next run its spin physics program and Primakoff program preparations, followed by its pion beam physics program, including pion polarizability. For pion polarizability, $\gamma\pi$ scattering will be measured via radiative pion scattering (pion Bremsstrahlung) in the nuclear Coulomb field: $\pi + Z \rightarrow \pi' + \gamma + Z$. A virtual photon from the Coulomb field of the target nucleus is scattered from the pion and emerges as a real photon accompanying the pion at small forward angles in the laboratory frame, while the target nucleus (in the ground state) recoils with a small transverse momentum kick p_t. The radiative pion scattering reaction is equivalent to $\gamma + \pi \rightarrow \gamma + \pi$ scattering for laboratory γ's of order 1 GeV incident on a target π at rest. The pion polarizabilities are determined by their effect on the shape of the measured $\gamma\pi$ Compton scattering angular distribution.

Significance:

The pion polarizabilities are key observables, and provide stringent tests of our understanding of chiral symmetry, its spontaneous breakdown, the role of explicit symmetry breaking in QCD, and consequently the very foundations of nuclear physics. The χPT effective Lagrangian, using data from radiative pion beta decay, predicts the pion electric and magnetic polarizabilities $\bar{\alpha}_\pi$ = -$\bar{\beta}_\pi$ = 2.7 $\pm$ 0.4. New high precision pion polarizability measurements via radiative pion scattering data from COMPASS will provide important new tests of this QCD chiral dynamics prediction.

[1] together with: F. Balestra, R. Bertini, M.P. Bussa, M. Colantoni, O. Denisov, A. Dolgopolov, M. Faessler, A. Ferrero, L. Ferrero, J. Friedrich, V. Frolov, R. Garfagnini, N. Grasso, V. Kolossov, R. Kuhn, A. Maggiora, M. Maggiora, A. Manara, Y. Mikhailov, V. Obraztsov, A. Olchevski, D. Panzieri, S. Paul, G, Piragino, J. Pochodzalla, V. Poliakov, A. Sadovski, M. Sans, L. Schmitt, H. Siebert, A. Skachkova, T. Walcher, A. Zvyagin

1 Scientific Background:

Pion polarizabilities will be measured at the CERN COMPASS experiment [1, 2, 3, 4, 5, 6], a new high priority approved spectrometer facility at CERN that uses muon and pion beams for studies of hadron structure and spectroscopy. The polarizabilities are obtained from measurements of the $\gamma\pi \rightarrow \gamma\pi$ gamma-pion Compton scattering. For the pion, chiral perturbation theory (χPT) leads to precision predictions for the polarizabilities [7, 8, 9]. Precision measurements of polarizabilities therefore subject the χPT techniques of QCD to new and serious tests.

1.1 Pion Polarizabilities via Primakoff Scattering

For the pion polarizability, $\gamma\pi$ scattering was measured (with large uncertainties) with 40 GeV pions [10] via radiative pion scattering (pion Bremsstrahlung) in the nuclear Coulomb field:

$$\pi + Z \rightarrow \pi' + \gamma + Z'. \tag{1}$$

In this measurement, the incident pion Compton scatters from a virtual photon in the Coulomb field of a nucleus of atomic number Z; and the final state γ and pion are detected in coincidence. The radiative pion scattering reaction is equivalent to $\gamma + \pi^- \rightarrow \gamma + \pi^-$ scattering for laboratory γ's of order 1 GeV incident on a target π^- at rest. It is an example of the well tested Primakoff formalism [11, 12] that relates processes involving real photon interactions to production cross sections involving the exchange of virtual photons.

In the 40 GeV radiative pion scattering experiments, it was shown experimentally [10] and theoretically [13] that the Coulomb amplitude clearly dominates, and yields sharp peaks in t-distributions at very small squared four momentum transfers (t) to the target nucleus $t \leq 6 \times 10^{-4}\,(\mathrm{GeV/c})^2$. Backgrounds from strong processes were low, and are expected to be even lower at the higher energy ($\sim$ 190 GeV) planned for the CERN COMPASS experiment.

All polarizabilities in this paper are expressed in units of 10^{-43} **cm**^{3}. The χPT 1-loop prediction [7, 8] for the pion polarizability is $\bar{\alpha}_\pi = -\bar{\beta}_\pi = 2.7 \pm 0.4$; with values $\bar{\alpha}_\pi = 2.4 \pm 0.5$; $\bar{\beta}_\pi = -2.1 \pm 0.5$, at two-loop [8]. Holstein [7] showed that meson exchange via a pole diagram involving the $a_1(1260)$ resonance provides the main contribution ($\bar{\alpha}_\pi$ = 2.6) to the polarizability. Xiong, Shuryak, Brown (XSB) [14] assuming a_1 dominance find $\bar{\alpha}_\pi$ = 1.8.

In fact, the $a_1(1260)$ width and the pion polarizability are related to an interesting question, which is whether or not one can expect gamma ray rates from the quark gluon plasma to be higher than from the hot hadronic gas phase in relativistic heavy ion collisions. XSB calculate photon production from a hot hadronic gas via the reaction $\pi^- + \rho^0 \rightarrow \pi^- + \gamma$. They assume that this reaction proceeds through the $a_1(1260)$. For $a_1(1260) \rightarrow \pi\gamma$, the experimental width [12] is $\Gamma = 0.64 \pm 0.25$ MeV. XSB [14] used an estimated radiative width Γ = 1.4 MeV, higher than the experimental value [12], as determined in the Primakoff reaction $\pi Z \rightarrow a_1 Z$, followed by $a_1^- \rightarrow \pi^-\rho$. It is with this estimated width that they calculate the pion polarizability to be $\bar{\alpha}_\pi$ = 1.8. COMPASS can experimentally check the a_1 dominance assumption of XSB via the inverse detailed balance Primakoff reaction $\pi Z \rightarrow a_1 Z$, and the consistency of the expected relationship of this radiative width and the pion polarizability [15].

For the kaon, χPT predicts [3, 7, 20] $\bar{\alpha}_{K^-}$ = 0.5 . The kaon polarizability measurements at COMPASS should complement those for pion polarizabilities for chiral symmetry tests away from the chiral limit. A more extensive study of kaon polarizabilities was given by Ebert and Volkov [16]. Until now, only an upper limit [17] at 90% confidence was measured (via energy shifts in heavy Z kaonic atoms) for the K^-, with $\bar{\alpha}_K \leq 200$.

1.2 Pion Polarizabilities

For the $\gamma\pi$ interaction at low energy, chiral perturbation theory (χPT) provides a rigorous way to make predictions via a Chiral Lagrangian having only renormalized coupling constants L_i^r [18] as empirical parameters. With a perturbative expansion of the effective Lagrangian, the method establishes relationships between different processes in terms of the L_i^r. For example, the radiative pion beta decay and electric pion polarizability are expressed as [7]:

$$F_A/F_V = 32\pi^2(L_9^r + L_{10}^r);\ \bar{\alpha}_\pi = \frac{4\alpha_f}{m_\pi F_\pi^2}(L_9^r + L_{10}^r); \tag{2}$$

where F_π is the pion decay constant, F_A and F_V are the axial vector and vector coupling constants in the decay, and α_f is the fine structure constant. The experimental ratio F_A/F_V = 0.45 $\pm$ 0.06, leads to $\bar{\alpha}_\pi$ = -$\bar{\beta}_\pi$ = 2.7 $\pm$ 0.4, where the error shown is due to the uncertainty in the F_A/F_V measurement [7, 9].

The pion polarizabilities deduced by Antipov et al. [10] in their low statistics experiment ($\sim$ 7000 events) were $\bar{\alpha}_\pi = -\bar{\beta}_\pi = 6.8 \pm 1.4 \pm 1.2$, with the analysis constraint that $\bar{\alpha}_\pi + \bar{\beta}_\pi = 0$, as expected theoretically [7]. The deduced polarizability value, not counting the large error bars, is some three times larger than the χPT prediction. **The available polarizability results have large uncertainties. There is a clear need for new and improved radiative pion scattering data.**

2 Research Goals and Expected Significance:

We studied the statistics attainable and uncertainties achievable for the pion polarizabilities in the COMPASS experiment, based on Monte Carlo simulations. We begin with an estimated $\sigma(Pb) = 0.5mb$ Compton scattering cross section per Pb nucleus and a total inelastic cross section per Pb nucleus of 0.8 barn. High statistics will allow systematic studies, with fits carried out for different regions of photon energy ω, Z^2, etc.; and polarizability determinations with statistical uncertainties lower than 0.1.

The expected pion beam flux is 2×10^7 pions/sec, while the spill structure provides a 5 second beam every 16 seconds. For pion polarizability, in 2 months of running at 100% efficiency, we obtain $3.2\times\ 10^{13}$ beam pions. We use a 0.8 % interaction length target, 3 mm Lead plate with target density $N_t = 10^{22}cm^{-2}$. The Primakoff interaction rate is then $R = \sigma(Pb) \cdot N_t = 5.\times\ 10^{-6}$. Therefore, in a 2 month run, one obtains 1.6×10^8 Primakoff polarizability events at 100% efficiency. Considering efficiencies for tracking (92%), γ detection (58%), accelerator and COMPASS operation (60%), analysis cuts to reduce backgrounds (75%), we estimate a global efficiency of ϵ(total)=24%, or $4.\times\ 10^7$ useful pion polarizability events per 2 month run. Prior to the data production run, time is also needed to calibrate ECAL2, to make the tracking detectors operational, to bring the DAQ to a stable mode, and for other contingencies. The above expected statistics in a two month data production run is a factor 6000 higher than the 7000 events of the previous pion polarizability Primakoff experiment.

We can also access kaon polarizabilities considering the approximately 1% kaon component of the beam One requires the CERN CEDAR Cerenkov beam detector for the kaon particle identification. Statistics of order $4. \times 10^5$ events would allow a first time determination of the kaon polarizability.

COMPASS provides a unique opportunity to investigate pion polarizabilities. Taking into account the very high beam intensity, fast data acquisition, high acceptance and good resolution of the COMPASS setup, one can expect from COMPASS the highest statistics and a 'systematics-free' data sample that includes many tests to control possible systematic errors.

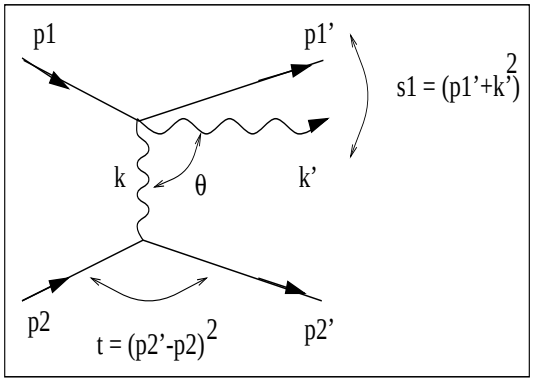

Figure 1: The Primakoff γ-hadron Compton process and kinematic variables (4-momenta): p1, p1′ = for initial/final hadron, p2, p2′ = for initial/final target, k, k′ = for initial/final gamma, and θ the scattering angle of the γ in the alab frame.

3 Detailed description of Research Program:

COMPASS is a fixed target experiment which will run primarily with a 160 GeV polarized muon beam and a 190 GeV pion beam. In order to achieve a good energy resolution within a wide energy range, COMPASS is designed as a two stage spectrometer with 1.0 Tm and 5.2 Tm conventional magnets. The tracking stations are composed of different detector types to cover a large area while achieving a good spatial resolution in the vicinity of the beam. Most of the tracking detectors operate on the principle of gas amplification, while some are silicon strip detectors. At the end of each stage, an electromagnetic and a hadronic calorimeter detects the energies of the gammas, electrons and hadrons. The calorimeters of the first stage and the EM calorimeter of the second stage have holes through which the beam passes.

We considered elsewhere in detail the beam, detector, and trigger requirements for polarizability studies in the CERN COMPASS experiment [3, 4, 5]. We describe here the pion polarizability measurements via the reaction $\pi^- + \mathrm{Z} \rightarrow \pi^{-'} + \gamma + \mathrm{Z}'$.

3.1 Monte Carlo Simulations

The setup we used for the Monte Carlo simulations was the official setup for the year 2001 run with the addition of three GEM stations and six silicon stations as projected for the year 2002 run. The additional detectors allow more precise tracking. We carried out the polarizability simulations using (1) the POLARIS event generator with (2) the CERN COMPASS GEANT (COMGEANT) package [19], whose output is a ZEBRA file with the information on the traces left by particles in detectors, (3) the CORAL COMPASS reconstruction and analysis library, structured as a set of modules: an input package is used to read the ZEBRA files produced by COMgeant, TraFFiC(TRAck Finding and FItting in Compass), calorimeter and RICH packages, a ROOT output package, the detector data decoding package, etc., and (4) the new CERN histograming and display and fit program ROOT. We use the terms *generated* and *reconstructed*, the first denoting the input physics events to COMgeant from POLARIS and the latter the output of CORAL which contains the reconstruction of these events in the the COMPASS spectometer.

POLARIS produces events of the type Eq. 1, based on the theoretical Primakoff $\gamma\pi$ Compton scattering cross section. The four-momentum of each particle is p1, p2, p1′, p2′, k, k′, respectively, as shown in Fig. 1. In the one-photon exchange domain, this reaction is equivalent to $\gamma + \pi \rightarrow \gamma' + \pi'$, and the four-momentum of the incident virtual photon is k = q = p2−p2′. We have therefore t=k^2 with t the square of the four-momentum

transfer to the nucleus, F(t) the nuclear form factor (essentially unity at small t, $\sqrt{s}$ the mass of the $\gamma\pi$ final state, and t_0 the minimum value of t to produce a mass $\sqrt{s}$. The momentum modulus $|\vec{k}|$ (essentially equal to p_T) of the virtual photon is in the transverse direction, and is equal and opposite to the momentum p_T transferred to the target nucleus. The pion polarizability is extracted via a fit of the theoretical cross section to the scattered γ angular distribution in the projectile (alab) rest frame. The total Primakoff cross section is computed by integrating numerically the differential cross section $\sigma(s,t,\theta)$ of Eq. 3 below for the Primakoff Compton process.

3.2 Primakoff $\gamma\pi$ Compton Event Generator

We describe the event generator for the radiative scattering of the pion in the Coulomb field of a nucleus [20]. In the pion alab frame, the nuclear Coulomb field of target M_Z effectively provides a virtual photon beam incident on a pion target at rest. We have for the variable $t=k^2=q^2\equiv M^2$, where t is the 4-momentum transferred to the nucleus, and M is the virtual photon mass. Since $t=2M_Z[M_Z\text{-}E(Z',lab)]<0$, the virtual photon mass is imaginary. To approximate real pion Compton scattering, the virtual photon should be taken to be almost real. For small t, the electromagnetic contribution to the scattering amplitude is large compared to meson and Pomeron (diffractive) exchange contributions. Radiative corrections for Primakoff scattering have been calculated to be very small [21].

The Primakoff differential cross section of the process of Eq. 1 in the alab frame may be expressed as [22]:

$$\frac{d^3\sigma}{dtd\omega d\cos\theta}=\frac{\alpha_f Z^2}{\pi\omega}\cdot\frac{t-t_0}{t^2}\cdot\frac{d\sigma_{\gamma\pi}(\omega,\theta)}{d\cos\theta}\cdot F^2(t), \tag{3}$$

where the $\gamma\pi$ cross section is given by:

$$\frac{d\sigma_{\gamma\pi}(\omega,\theta)}{d\cos\theta}=\frac{2\pi{\alpha_f}^2}{m_\pi^2}\cdot\{F_{\gamma\pi}^{pt}(\theta)+\frac{m_\pi\omega^2}{\alpha_f}\cdot\frac{\bar{\alpha}_\pi(1+\cos^2\theta)+2\bar{\beta}_\pi\cos\theta}{(1+\frac{\omega}{m_\pi}(1-\cos\theta))^3}\}. \tag{4}$$

Here, $t_0=(m_\pi\omega/p_b)^2$, with p_b the incident pion beam momentum in the laboratory, θ the scattering angle of the real photon relative to the incident virtual photon direction in the alab frame, ω the energy of the virtual photon in the alab frame, Z the nuclear charge, m_π the pion mass, α_f the fine structure constant, F(t) is the nuclear electromagnetic form factor (approximately unity in the range $t<2.5\times10^{-4}GeV^2$), and $\bar{\alpha_\pi}$, $\bar{\beta}_\pi$ the pion electric and magnetic polarizabilities. The energy of the incident virtual photon in the alab (pion rest) frame is:

$$\omega\sim(s-{m_\pi}^2)/2m_\pi. \tag{5}$$

For COMPASS, this radiative pion scattering reaction is then equivalent to $\gamma+\pi\rightarrow\gamma+\pi$ scattering for laboratory γ's with energy of order $\omega=1GeV$ incident on a target π at rest. The function $F_{\gamma\pi}^{pt}(\theta)$ describing the Thomson cross section for γ scattering from a point pion is given by:

$$F_{\gamma\pi}^{pt}(\theta)=\frac{1}{2}\cdot\frac{1+\cos^2\theta}{(1+\frac{\omega}{m_\pi}(1-\cos\theta))^2}. \tag{6}$$

From Eq. 4, the cross section depends on $(\bar{\alpha}_\pi+\bar{\beta}_\pi)$ at small θ, and on $(\bar{\alpha}_\pi-\bar{\beta}_\pi)$ at large θ. A precise fit of the theoretical cross section (Eq. 3-6) to the measured angular distribution of scattered γ's, allows one to extract the pion electric and magnetic polarizabilities. Fits will be done for different regions of ω for better understanding of the systematic uncertainties. We will carry out analyses with and without the dispersion sum rule constraint [7] that $\bar{\alpha}_\pi+\bar{\beta}_\pi\approx0.4$. We can achieve a significantly smaller uncertainty for the polarizability by including this constraint in the fits.

The event generator produces events in the alab frame, characterized by the kinematical variables t, ω and $\cos\theta$, and distributed with the probability of the theoretical Compton Primakoff cross section (Eq. 3-6). Then, the $\gamma\pi$ scattering kinematics are calculated. The virtual photon incident along the recoil direction $\vec{k}/|\vec{k}|$, is scattered on the pion "target", and emerges as a real photon with energy/momentum $\omega'/|\vec{k}'|$ at an angle θ:

$$\omega' = \frac{\omega(1 + \frac{\omega^2 - |\vec{k}|^2}{2m_\pi\omega})}{1 + \frac{\omega}{m_\pi}(1 - \frac{|\vec{k}|}{\omega}\cos\theta)} \tag{7}$$

The photon azimuthal angle around the recoil direction is randomly generated using a uniform distribution. The four-vector components of all reaction participants (pion, photon and recoil nucleus) are then calculated in the alab frame. The azimuthal angle of the recoil nucleus is also randomly generated by a uniform distribution. Finally, the reaction kinematics are transformed to the lab frame by a Lorentz boost.

For the measurement of the pion polarizabilities, one must fit the theoretical cross section (3-6) to measured distributions, after correcting for acceptances. The sensitivity to the polarizability increases with increasing ω energy and at back angles. A convenient method is to use the $\cos\theta$ distribution integrated over t and for different ranges of ω, since this shows clearly the sensitivity to the polarizability.

3.3 Design of the Primakoff Trigger

The small Primakoff cross section and the high statistics required for extracting polarizabilities require a data run at high beam intensities and with good acceptance. This sets the main requirements for the trigger system: (1) to act as a "beam killer" by accepting only Primakoff scattered pions, and suppressing the high rate background associated with non-interacting beam pions, (2) to avoid cutting the acceptance at the important γ back angles in the alab frame, where the hadron polarizability measurement is most sensitive, (3) to cope with background in the γ calorimeter from low energy γ's or delta electrons.

We achieve these objectives via a COMPASS Primakoff trigger that makes use of a beam veto, a target recoil detector, the calorimeters and various hodoscopes. A coincidence is required of the scattered pion with a γ measured in the ECAL2 calorimeter. We demonstrated the feasibility and field operation of such a trigger, via Monte Carlo simulations [3, 4, 5, 24, 25, 26] and via beam tests with the COMPASS spectrometer [23].

For the reaction given in Eq. 1, for illustration at 300 GeV pion beam energy, the laboratory outgoing γ's are emitted within an angular cone of within 5 mrad, and the corresponding outgoing π's are emitted within 2 mrad. Most events have γ energies between $0 - 280$ GeV, and π energies between $20 - 300$ GeV.

Our MC shows that we lose very little polarizability information by applying an "energy cut" trigger condition that rejects events with the outgoing pion energy having more than 240 GeV. Correspondingly, the final state γ has less than 60 GeV. The 240 GeV cut acts as a beam killer. The 60 GeV cut will also be very effective in reducing the γ detector (ECAL2) trigger rate, since a large part of the background γ rate is below 60 GeV.

The polarizability insensitivity to these cuts results from the fact that the most forward (in alab frame) Compton scattering angles have the lowest laboratory γ energies and largest laboratory angles. In addition, the cross section in this forward alab angle range is much less sensitive to the polarizabilities. This is seen from Eq. 4, since with $\bar{\alpha}_\pi + \bar{\beta}_\pi \approx 1$ used in our MC, the polarizability component is small at forward compared to back angles. The acceptance is reduced by the energy cut for the forward alab angles (shown in Fig. 2), but is unaffected at the important alab back angles. Summarizing, the pion and γ energy constraints at the trigger level fulfill the "beam killer" requirement and at the same time remove backgrounds coming from low energy γ's, delta electrons, and e^+e^- pairs incident on ECAL2, etc. Similar results are obtained for the effectiveness of an energy loss trigger for simulations carried out at 190 GeV pion beam energy.

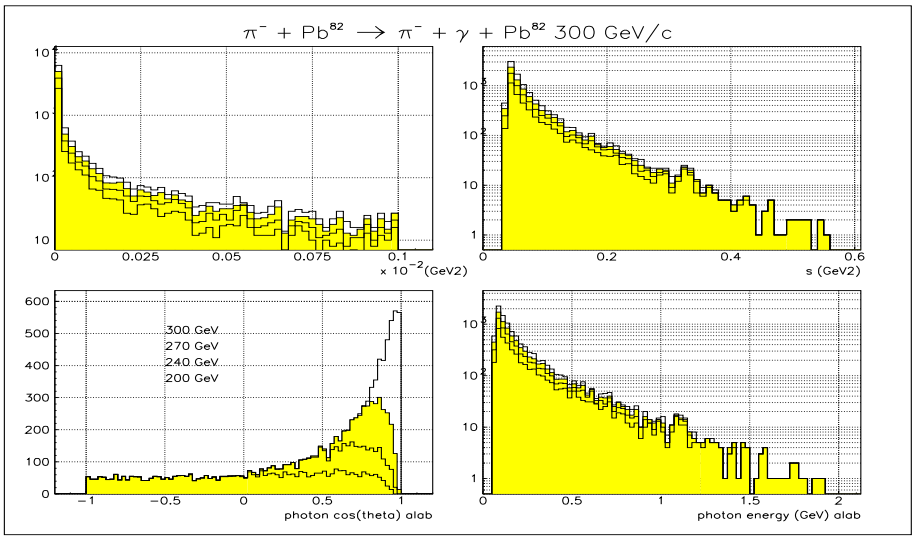

Figure 2: MC simulation showing the acceptance of the $\gamma\pi \rightarrow \gamma\pi$ reaction in terms of the invariant four momentum transfer t to the target,the squared invariant energy s of the final state $\gamma\pi$, the angular distribution versus $\cos(\theta)$ with θ the γ scattering angle in the alab frame, and the virtual photon energy ω in the alab frame. The overlayed spectra correspond to different cuts on the final state π momentum.

Test beam studies for the trigger were performed in Sept. 2000 [23]. The setup for the test beam was the following (see figure 3): a beam counter upstream of the target (S); a beam veto counter (beam killer) in front of ECAL2, covering the hole for the deflected primary beam (B); a hodoscope 80 cm × 96 cm, situated in front of ECAL2 (H), displaced horizontally by 20 cm from the position of the deflected beam; a veto system around the target and the electromagnetic calorimeter (ECAL2).

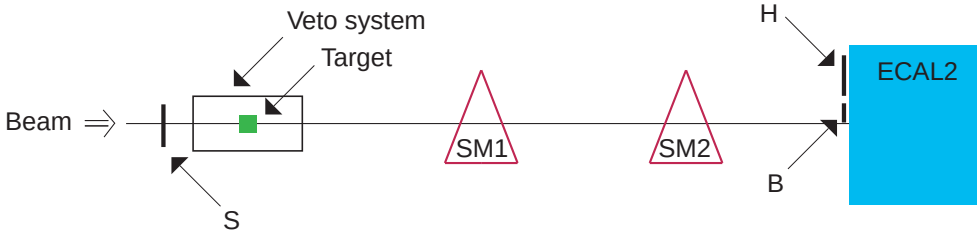

Figure 3: Trigger setup for the Primakoff measurement in COMPASS. It consits of a beam counter (S), beam veto counter (B), a hodoscope (H), a veto system around the target and the electromagnetic calorimeter (ECAL2).

According to the signature of the reaction, a beam particle is expected in S. Particles scattered by the target, should give a signal in H. No signal should be registered in the beam killer B, but a highly energetic photon should be detected in ECAL2. The test beam demonstrated that an acceptable rate for the trigger can be achieved. The requirements to achieve this rate are the following: the coincidence between the energy deposition in the ECAL2 above a threshold of 0.2 to $0.3 \times E_{beam}$ and the existence of a charged particle in the corresponding acceptance of H. The use of the beam killer B and of the veto counter does not improve much the rate reduction. The target veto could be used offline to reject background reactions with large momentum transfer to the target.

Some interesting numbers that are quoted include the following: from a beam intensity of $6 \cdot 10^6$/spill with a

3 mm lead target, the trigger rate was found to be 2.5 $\times 10^5$/spill. The trigger gives a reduction factor of 24. The idea of the trigger is not to reduce too strongly the number of events since this will be done offline when analysing the events. The size of the hodoscope needed to cover the acceptance of the simulated scattered pions was calculated by plotting the simulated hit distribution of the scattered pions at the position where the hodoscope will be situated. Figure 4 shows that the size needed for the hodoscope is 1 meter in horizontal direction and 40 cm. in vertical direction.

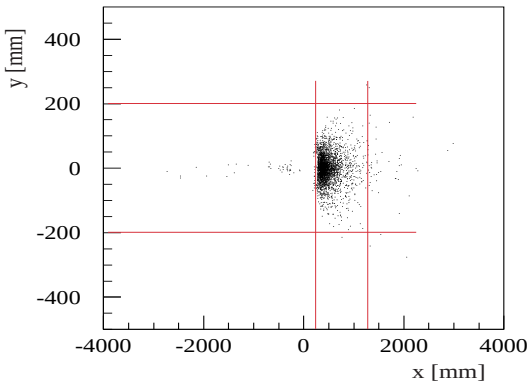

Figure 4: Simulated hit distribution of the scattered pion at 30 meters from the target. The lines indicate the possible size of the trigger hodoscope.

3.4 Beam Requirements

In COMPASS, two beam Cherenkov detectors (CEDARS) far upstream of the target provide $\pi/K/p$ particle identification (PID). The incoming hadron momentum is measured in the beam spectrometer. Before and after the target, charged particles are tracked by high resolution silicon tracking detectors. The measurement of both initial and final state momenta provides constraints to identify the reaction. The final state pion and γ momenta are measured downstream in the magnetic spectrometer and in the γ calorimeter, respectively. These measurements allow a precise determination of the small p_T kick to the target nucleus, the main signature of the Primakoff process, and the means to separate Primakoff from meson exchange scattering events.

We can get quality statistics for the pion study with high beam intensities at the CERN SPS. We will take data with different beam energies and targets, with both positive and negative beams, as part of efforts to control systematic errors. We can take data with the muon beam also for muon Primakoff Compton scattering, to test our methodologies, and to provide a comparison later of pion Primakoff Compton scattering (depending on pion polarizability) with respect to muon Primakoff Compton scattering (with zero muon polarizability).

3.5 Target and Target Detectors

The target platform is moveable and allows easy insertion of a normal solid state target, e. g. a cylindric lead plate 40 mm in diameter and 3 mm in width. We also plan Primakoff scattering on nuclei with Z$<$ 82 to check the expected Z^2 cross section dependence. We use silicontracking detectors before and immediately after the targets. These are essential for Primakoff reactions as the scattering angle has to be measured with a precision of order 100 μrad, because it contains much of the information. We veto target break-up events by a target veto recoil detector, and by selecting low-t events in the off-line analysis. The recoil detector is currently developed and tested. A particle momentum of about 100 MeV should be sufficient to trigger a veto coincidence in its scintillator and Lead glass layers. This veto will limit the angular acceptance to about

100 mrad to reject events where fragments of the nucleus or particles produced in diffractive processes leave the target with bigger angles to the beam axis.

3.6 The Magnetic Spectrometer and the t-Resolution

We achieve good momentum resolution for the incident and final state pions and γ's, and therefore good four momentum t-resolution. The relative momentum resolution for π^- with all interactions accounted for is 1% for energies above 35 GeV and up to 2.5% below this mark. The angular resolution in a single coordinate for a pion of momentum p is 7.9 mrad-Gev/p. All generated pions with energy greater than 2 GeV were in the acceptance of the spectrometer, the reconstruction efficiency with interactions enabled is 92%.

The angular resolution for the final state π is controlled by minimizing the multiple scattering in the targets and detectors. With a lead target of 1% interaction length (2 g/cm^2, 30% radiation length), multiple Coulomb scattering (MCS) of the beam and outgoing pion in the target gives an rms angular resolution of order 40 μrad, small compared to the intrinsic tracking detector angular resolution. The target contributes to the resolution of the transverse momentum p_T via the p_T generated through MCS. Considering $t = p_T^2$, including all other effects [3, 4, 5], we aim for a p_T resolution less than 15 MeV, corresponding to Δt better than $\approx 2.5 \times 10^{-4}$ GeV^2.

This resolution will allow an effective t-cut to minimize contributions to the data from diffractive processes. The goal is achievable, based on the t distributions measured at a 200 GeV low statistics, high resolution experiment for $\pi^- Z \rightarrow \pi^- \pi^0 Z$ [11] and $\pi^- Z \rightarrow \pi^- \gamma Z$ [12] Primakoff scattering at 200 GeV at FNAL. The t distribution of the $\pi^- \rightarrow \pi^- \gamma$ data agrees well with the Primakoff formalism out to t = 10^{-3} GeV^2, which indicates that the data are indeed dominated by Coulomb production. Minimum material (radiation and interaction lengths) in COMPASS will also give a higher acceptance, since that allows γ's to arrive at ECAL2 with minimum interaction losses, and minimum e^+e^- backgrounds.

3.7 The γ Calorimeter ECAL2

The position resolution in the second γ calorimeter ECAL2 for the photon is 1.0 mm corresponding to an angular resolution of 30 μrad. In the interesting energy range the energy resolution is better than 1% after taking into account the leakage into the hadron calorimeter HCAL. The photon acceptance is 98% due to the beam hole of ECAL2 while the reconstruction efficiency is 58% as a result of pair production within the spectrometer.

This γ detector is equipped with 3.8 by 3.8 cm^2 GAMS lead glass blocks to make a total active area of order 1.5 m diameter. The central area needed for the polarizability measurement is only 30×30 cm^2, and is already completely instrumented with modern ADC readouts.

The p_T kicks of the COMPASS magnets are 0.45 GeV/c for SM1 (4 meters from target) and 1.2 GeV/c for SM2 (16 meters from target). The fields of both magnets are set *additive* for maximum deflection of the beam from the zero degree (neutral ray) line. We thereby attain at least 10 cm for the distance between the zero degree line and the hole edge. This is important since the Primakoff γ's are concentrated around the zero degree line and a good γ measurement requires clean signals from 9 blocks, centered on the hit block. From MC simulations, the number of Primakoff scattered pions below 40 GeV is less than 0.3%, so that 40 GeV pions are about the lowest energy of interest.

4 Simulation Results for 190 GeV Pion Beam

The most recent COMPASS Primakoff polarizability simulation results [24, 25, 26] are given now. We evaluated the single particle detection properties of the COMPASS spectrometer. The key results are a momentum resolution for pions of 1% above 35 GeV and up to 2.5% below 35 GeV accompanied by an angular resolution of 7.9 mrad GeV$/p$ and an energy resolution for photons of 1.5% above 90 GeV accompanied by an angular resolution of 30 μrad. The photon reconstruction inefficiency is given by the conversion probability before leaving the second spectrometer magnet; the corresponding efficiency is 58%. The single pion reconstruction efficiency is about 92%.

We describe the results of the simulation of Primakoff Compton scattering and of hadronic backgrounds. We study the influence of the COMPASS detector resolutions and reconstruction algorithms on the extraction of the polarizabilities. We achieve this via a simulation of Primakoff Compton scattering of π^- on Lead at a beam energy of 190 GeV at five different pairs of $\bar{\alpha}$ and $\bar{\beta}$ polarizability parameters with a total statistics of five times 620,000 events, each sample corresponding to the analyzed events from roughly a day of COMPASS data taking.

The following cuts are used to recognize Primakoff events: there has to be a photon hit in the ECAL2 above a certain energy and a negative charged track which carries the complementary energy. The cut on the photon energy has to be well above the energy deposition of hadrons in the electromagnetic calorimeter that is of the order of some GeV. In order to select the so-called "hard events" with most information on the pion polarizabilities, this cut is raised to 30–50% of the beam energy. In this simulation a cut on the photon energy at 90 GeV was implemented in the generator, so it was natural to use 80 GeV in the reconstruction. The energy window for the sum of pion and photon was set to 180–196 GeV to allow for the longitudinal energy leakage of ECAL2. The figures 5-8 were all produced only with the events that were left after applying these two cuts.

The reconstructed count rates have to be corrected for the inefficiency of the detector before fitting the cross section. The data of all five samples are merged to calculate the dependence of the reconstruction efficiency on the photon energy in the laboratory frame. Fig. 5 shows the generated and—with the cuts applied—the reconstructed photon energy in the laboratory frame, fig. 6 shows the corresponding efficiency with fit parameters. As expected from our studies of single photon and pion efficiencies, the overall efficiency is between 50-55%. Fig. 7 shows the beam energy distribution used in the simulation.

Compared to the generated $t = \mathsf{q}^2$ distribution, the reconstructed q^2 is smeared out due to the transverse momentum transfer error induced by angle reconstruction errors of the final state. For example, quadratically adding the errors for 110 GeV photon energy and 80 GeV pion momentum yields an error of 15 MeV. Nevertheless the rise is steep enough to permit a cut at $-\mathsf{q}^2 < 1000\ \mathrm{MeV}^2$, as seen in Fig. 8. Such a cut only reduces the efficiency by 6%.

We studied the efficiency for the selected events with small t and where the sum of the energy of the π^- and the γ is, within some resolution, equal to the energy of the beam. We found that this efficiency was independent of t, with no bias by the acceptance of the detector. Regardless of the cut in t, the important shape of the $\gamma\pi$ angular distribution is not affected.

4.1 Retrieving the polarizabilities

The generated and reconstructed four-momenta are transformed to the projectile (alab) frame. The fit is performed using the ROOT interface to the MINUIT package. To get the reconstructed differential cross section the event rates had to be corrected for the inefficiency of the detector. We observe that $\overline{\alpha}$ and $\overline{\beta}$ are anti-correlated, with the consequence that $\overline{\alpha} + \overline{\beta}$ is determined with a much smaller error than $\overline{\alpha} - \overline{\beta}$. The polarizability effect is proportional to $\overline{\alpha} + \overline{\beta}$ for $\cos\theta = 1$ and $\overline{\alpha} - \overline{\beta}$ for $\cos\theta = -1$, increasing with the photon

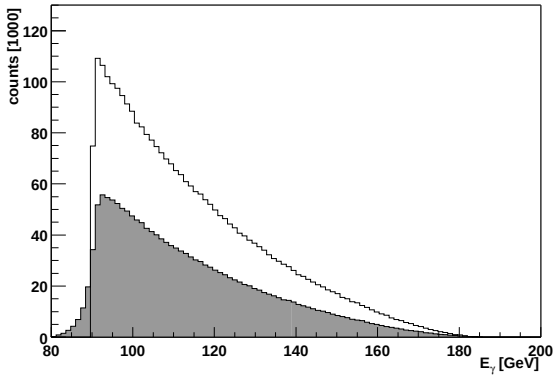

Figure 5: generated (white) and reconstructed (shaded) photon energy in the laboratory frame. The data of all five samples is merged ($2.9 \cdot 10^6$ events)

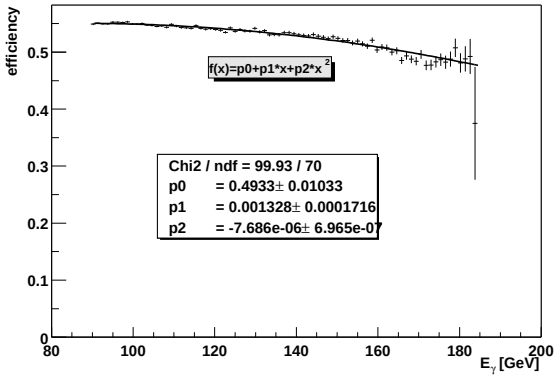

Figure 6: reconstruction efficiency vs. photon energy in the laboratory frame. The error bars are the binomial errors corresponding to the generated statistics shown in the left hand plot

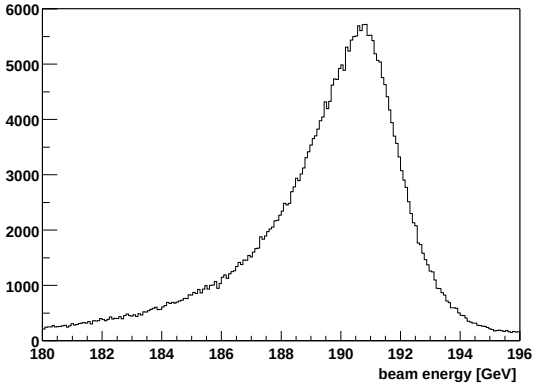

Figure 7: reconstructed beam energy

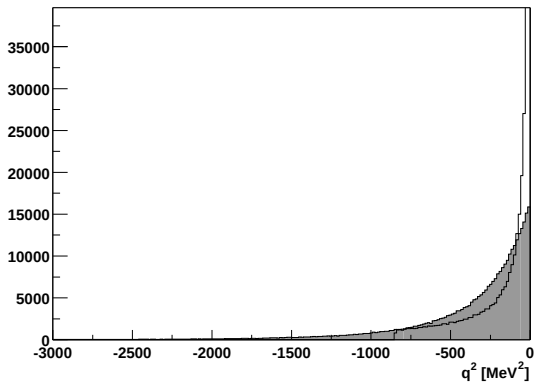

Figure 8: generated (white) and reconstructed (shaded) q^2

energy like ω^2. So $\overline{\alpha} - \overline{\beta}$ is mostly determined in the region with least events while $\overline{\alpha} + \overline{\beta}$ is better known because the cross section has a steep rise towards positive $\cos\theta$.

We carried out fits to determine the polarizabilities for each sample of 620,000 simulated events, each sample corresponding to different ($\overline{\alpha}$,$\overline{\beta}$) pairs. Reducing the statistical errors by 8, scaling to the assumed 4. $\times 10^7$ events, we estimate the statistical uncertainties for the two month COMPASS run to be about 0.05 for $\overline{\alpha}$ and $\overline{\beta}$, 0.01 for $\overline{\alpha} + \overline{\beta}$ and 0.1 for $\overline{\alpha} - \overline{\beta}$. Including systematic uncertainties, we aim to achieve better than 0.4 uncertainties in $\overline{\alpha}$ and $\overline{\beta}$.

4.2 The hadronic background

To investigate the corruption of the measured Primakoff cross section by hadronic background events, a large sample of minimum bias events was produced with the Fritiof pion-Nucleus event generator. The analysis of 4.5×10^6 events by the exact process described above accepts only 34 events, 27 of them were in the fit range for the polarizabilities [25].

As Fritiof only simulates hadronic interaction the mechanism for accepting some of the events is the production of π^0 or η. Because of the cut on the total energy sum of the pion and the photon, most of this background is rejected, as the remaining particles also receive their part of the energy. One may tighten this cut because the background would be much more affected than the real events.

The generated final state in all 34 cases contains a nucleon. This suggests that the nucleus was disintegrated in the reaction. The fragments are tracked by COMgeant, but there is no single particle ID to label them. Thus, they unfortunately are not part of the list of particles emerging from the primary vertex. Every event contains particles with polar angles bigger than 20 deg and a target recoil would see some of those events not stopped inside the target.

The overall signal to noise ratio for hadronic background can be estimated from the ratio of the cross sections and the background suppression. The hadronic interaction length of Lead of 194 g cm^{-2} corresponds to a cross section of 1.77 barn, the suppression factor of 26/4500000 reduces this to 10 μbarn. This has to be compared to the cross section of Primakoff Compton scattering—with a produced photon energy of at least 90 GeV—of about 500 μbarn. The ratio of 50:1 will be further improved by the inclusion of the target recoil veto and by a more sophisticated kinematics reconstruction.

5 Conclusions

COMPASS is on track to measure the $\gamma\pi$ Compton scattering cross sections, as a central part of its Primakoff physics program, thereby enabling determinations of the pion polarizabilities. The experiment will allow serious tests of χPT; and of different available polarizability calculations in QCD.

6 Acknowledgments

This research was supported in part by the Israel Science Foundation founded by the Israel Academy of Sciences and Humanities.

References

[1] International Workshop on Hadron Structure and Hadron Spectroscopy, Trieste, Italy, Feb. 2002, http://www.ts.infn.it/conferences/iwts2002/

[2] F. Bradamante, S. Paul et al., CERN Proposal COMPASS, http://wwwcompass.cern.ch/, CERN/SPSLC 96-14, SPSC/P297; CERN/SPSLC 96-30, SPSC/P297, Addendum 1; http://www-nuclear.tau.ac.il/∼murraym/primaphysreps.html

[3] M. A. Moinester, V. Steiner, Pion and Kaon Polarizabilities and Radiative Transitions, Proc. 'Chiral Dynamics Workshop' U. Mainz, Sept. 1997, hep-ex/9801008.

[4] M. A. Moinester, V. Steiner, S. Prakhov, Hadron-Photon Interactions in COMPASS, Proc. XXXVII Meeting on Nuclear Physics, Bormio, Italy, Jan. 1999, hep-ph/9910039

[5] M. A. Moinester, Pion Polarizabilities and Hybrid Meson Structure at COMPASS, Contribution to the APS DNP Town Meeting on Electromagnetic & Hadronic Physics, Dec. 2000, Newport News, Va., hep-ex/0012063

[6] A. Olchevski, M. Faessler, M. A. Moinester, Experimental Requirements for COMPASS Initial Primakoff Physics Program, COMPASS Collaboration Meeting presentations, 1999-2002.

[7] B. R. Holstein, *Comments Nucl. Part. Phys.* **19**, 239 (1990).

[8] U. Burgi, Nucl. Phys. B479 (1996) 392; Phys. Lett. B377 (1996) 147.

[9] D. Babusci, S. Bellucci, G. Giordano, G. Matone, A. M. Sandorfi, M. A. Moinester, *Phys. Lett.* B **277**, 158 (1992).

[10] Yu. M. Antipov et al., *Phys. Lett.* B **121**, 445 (1983), *Z. Phys.* C **26**, 495 (1985).

[11] T. Jensen et al., *Phys. Rev.* D **27**, 26 (1983).

[12] M. Zielinski et al., *Phys. Rev. Lett.* **52**, 1195 (1984).

[13] A. S. Galperin et al., *Sov. Jour. Nucl. Phys.* **32**, 545 (1980).

[14] L. Xiong, E. Shuryak, G. Brown, *Phys. Rev.* D **46**, 3798 (1992).

[15] M. A. Moinester, Pion Polarizability, Radiative Transitions, and Quark Gluon Plasma Signatures, Chiral Dynamics Workshop, M.I.T., July 1994, hep-ph/9410215.

[16] D. Ebert, M. K. Volkov, Phy. Atom. Nucl. 60 , 796 (1997).

[17] G. Backenstoss et al., *Phys. Lett.* B **43**, 431 (1973).

[18] J. Gasser and H. Leutwyler, *Nucl. Phys.* B **250**, 465 (1985).

[19] V. Alexakhine et al., COMPASS GEANT (COMGEANT), http://valexakh.home.cern.ch/valexakh/wwwcomg/index.html

[20] M. Buenerd, Nucl. Instr. Meth. A136 (1995) 128; V. Steiner, M. A. Moinester, M. Buenerd, POLARIS, A Monte Carlo event generator for polarizability experiments, 1995, unpublished.

[21] A. Akhundov, S. Gerzon, S. Kananov, M.A. Moinester, Z. Phys. 66C (1995)279.

[22] N. I. Starkov et al. *Sov. Jour. Nucl. Phys.* **36**, 1212 (1982).

[23] A Sadovski et al., Test beam studies for a trigger for a Primakoff measurement, COMPASS collaboration meeting, Oct. 2000, Dubna, Russia.

[24] M. Sans Merce, Ph.D. thesis, Ludwig Maximilians University, Munich, 2001.

[25] R. Kuhn, Diploma thesis, Technical University, Munich, 2001.

[26] M. Colantoni et al., Proc. XL Meeting on Nuclear Physics, Bormio, Italy, Jan. 2002.

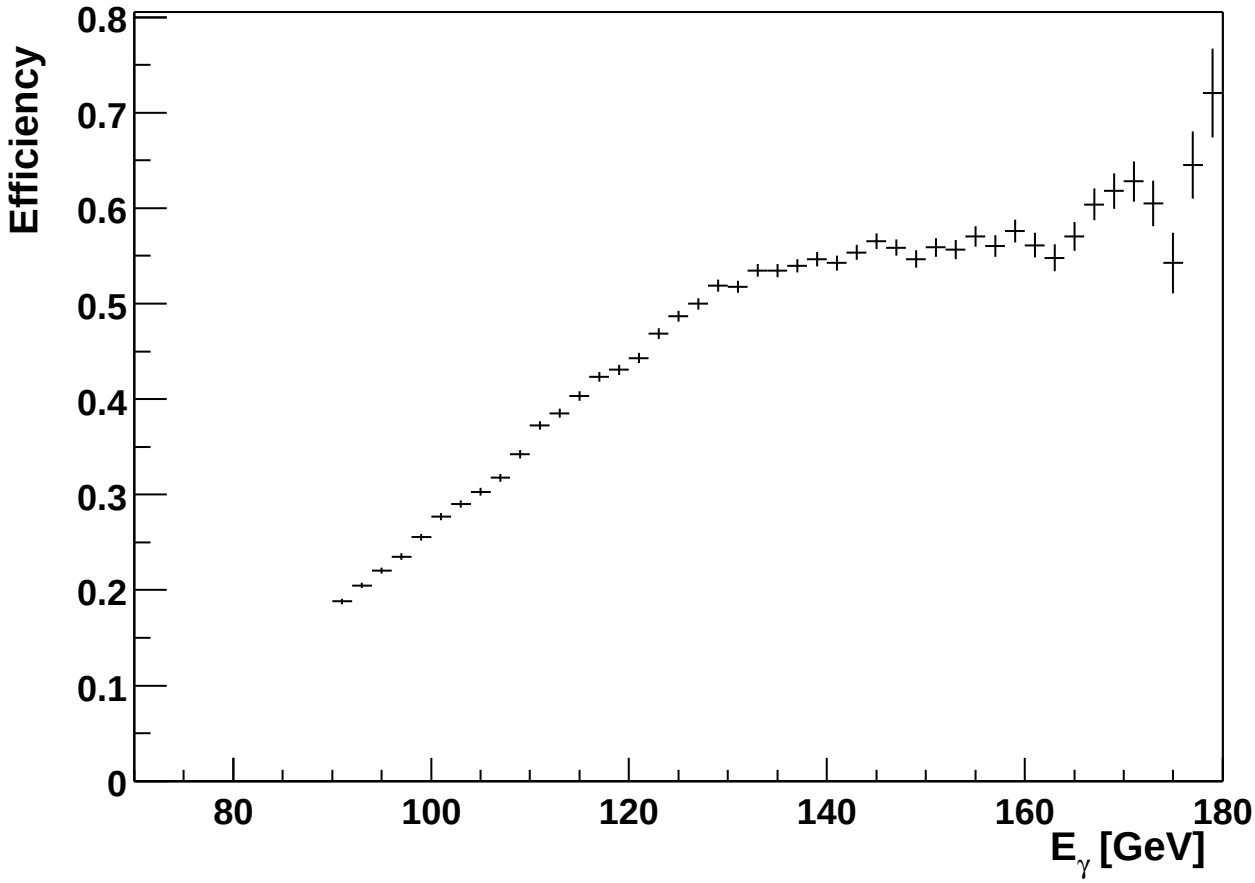
Efficiency
0.8
0.7
0.6
0.5
0.4
0.3
0.2
0.1
0
80
100
120
140
160
180
E_γ [GeV]

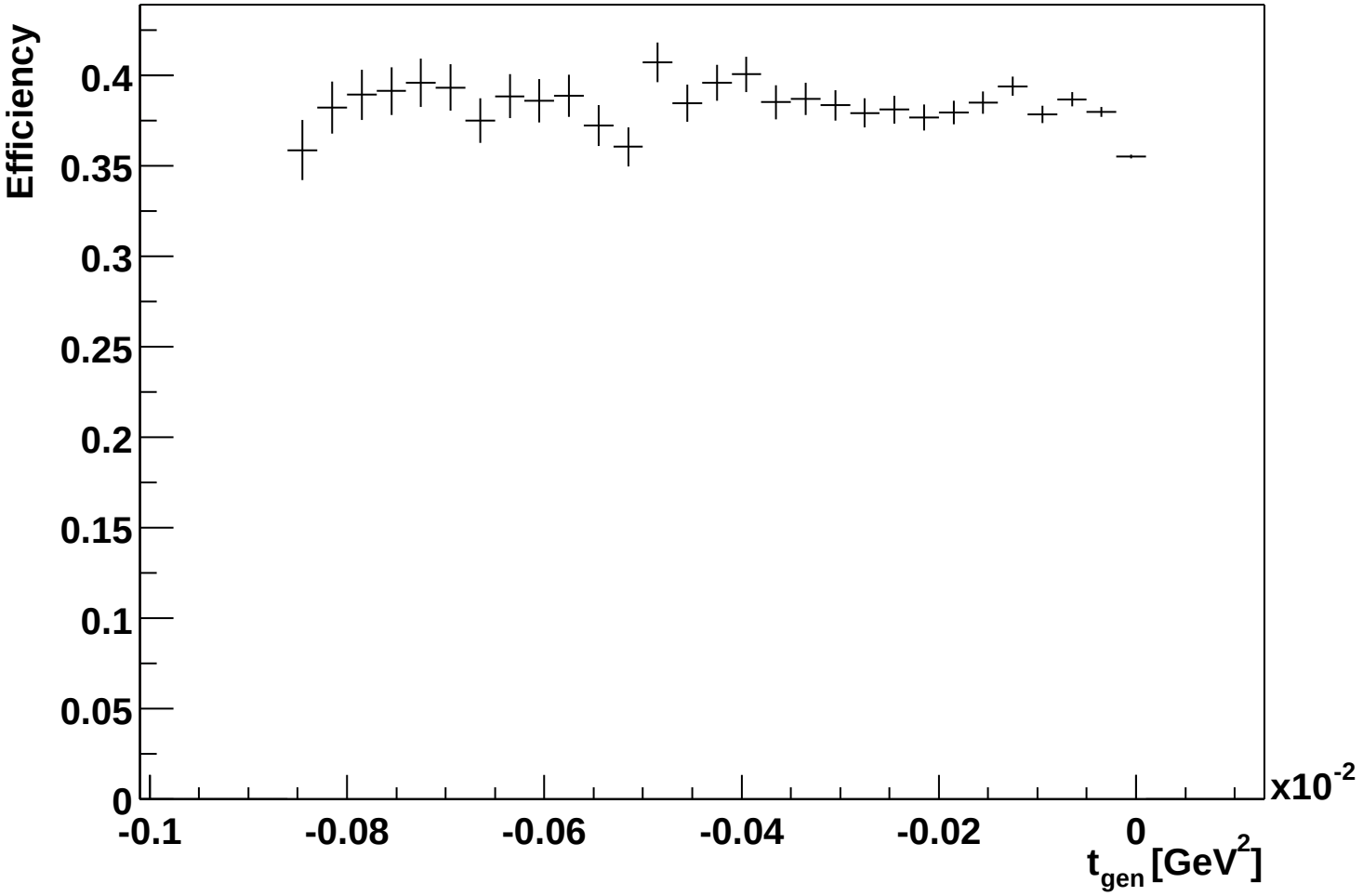
Efficiency
0.4
0.35
0.3
0.25
0.2
0.15
0.1
0.05
0
-0.1
-0.08
-0.06
-0.04
-0.02
0
x10^-2
t_gen [GeV^2]

$\pi^- + Pb^{82} \rightarrow \pi^- + \gamma + Pb^{8}$

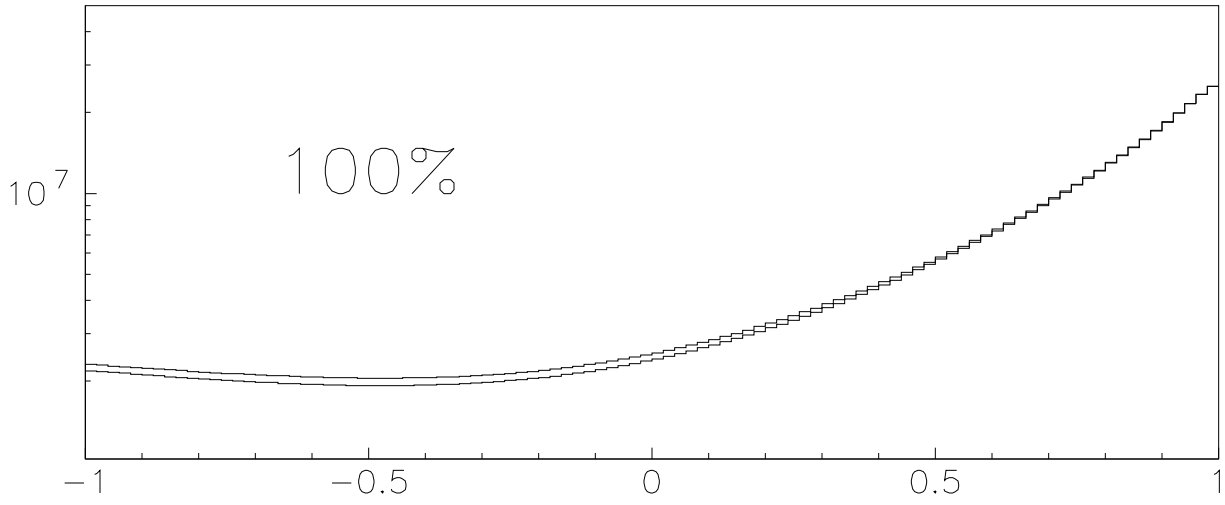

XS vs CTH * AH=BH=0 * ephot = 70.−2027.

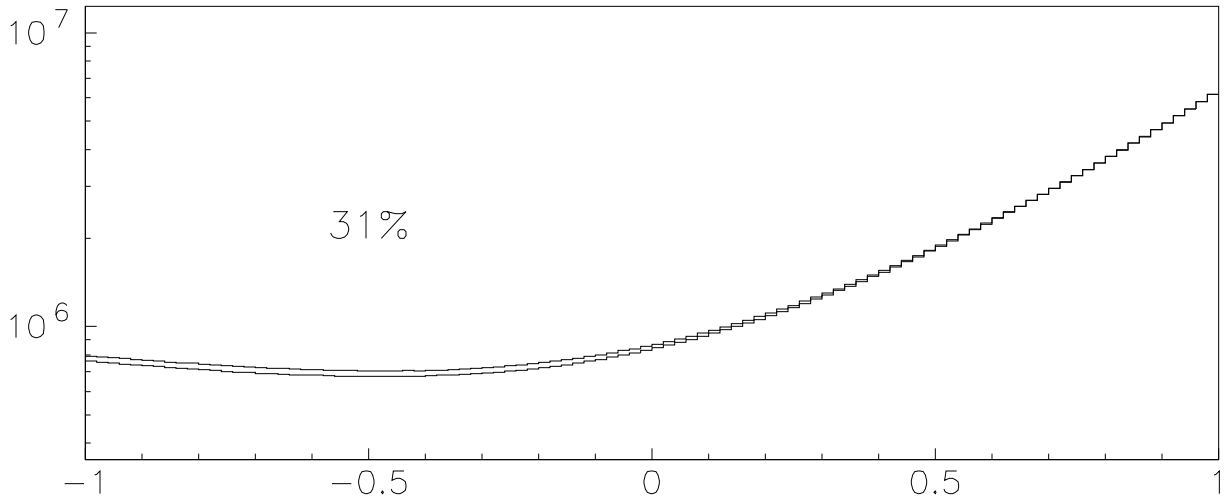

XS vs CTH AH=BH=0 * ephot = 100.− 170.

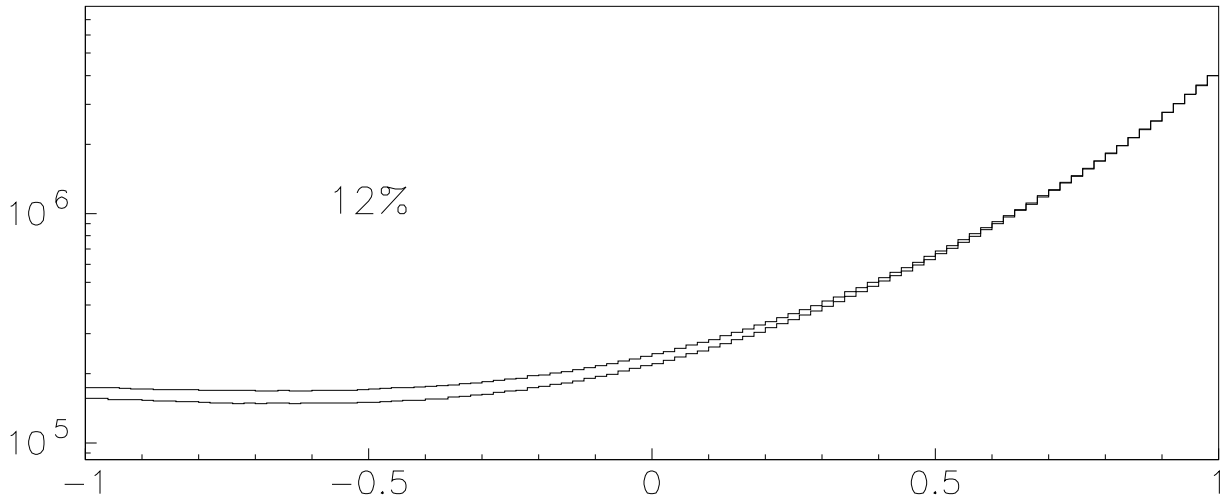

XS vs CTH AH=BH=0 * ephot = 230.− 350.

$\pi^- + Pb^{82} \rightarrow \pi^- + \gamma + Pb^{8}$

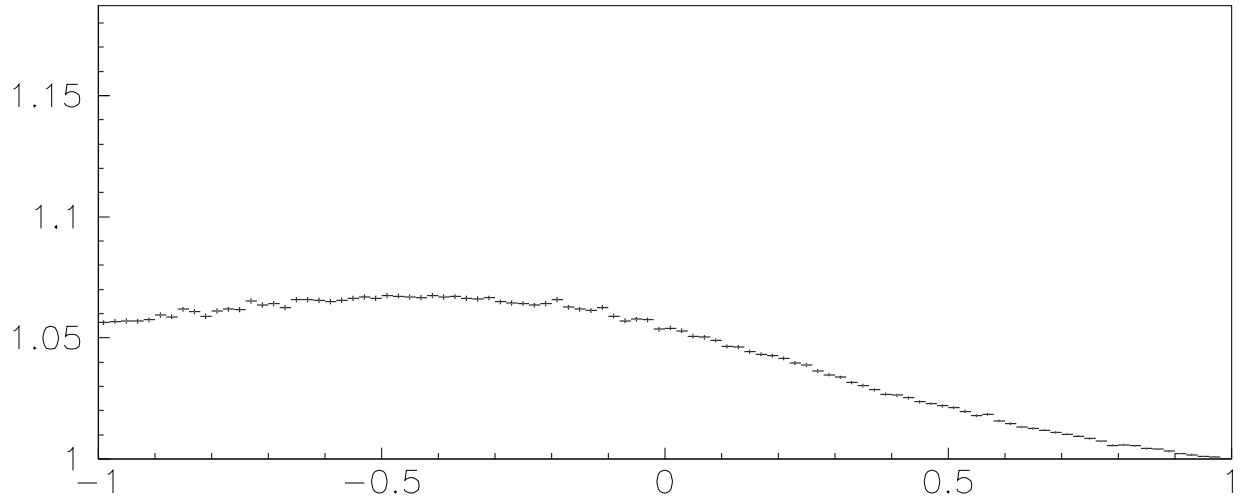

XS vs CTH * AH=BH=0 * ephot = 70.−2027.

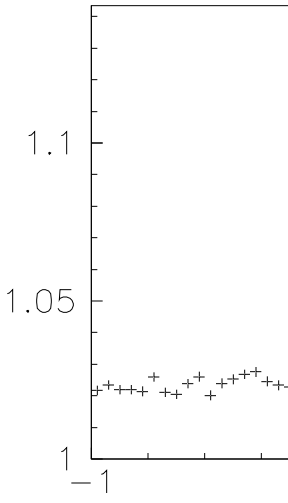

XS

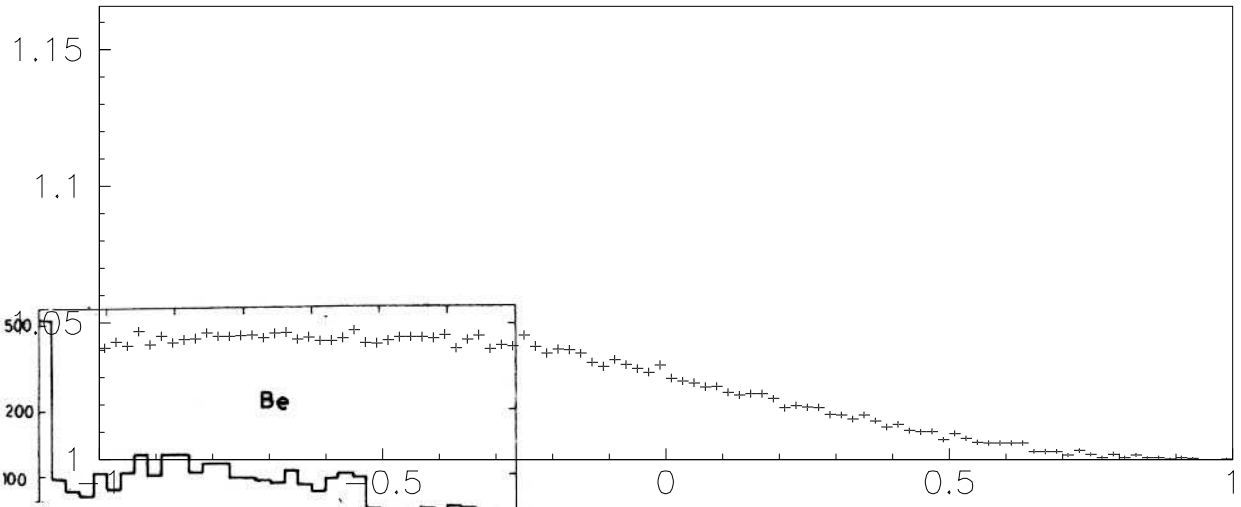

XS vs CTH AH=BH=0 * ephot = 100.− 170.

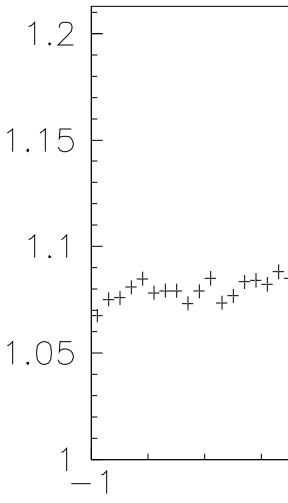

XS

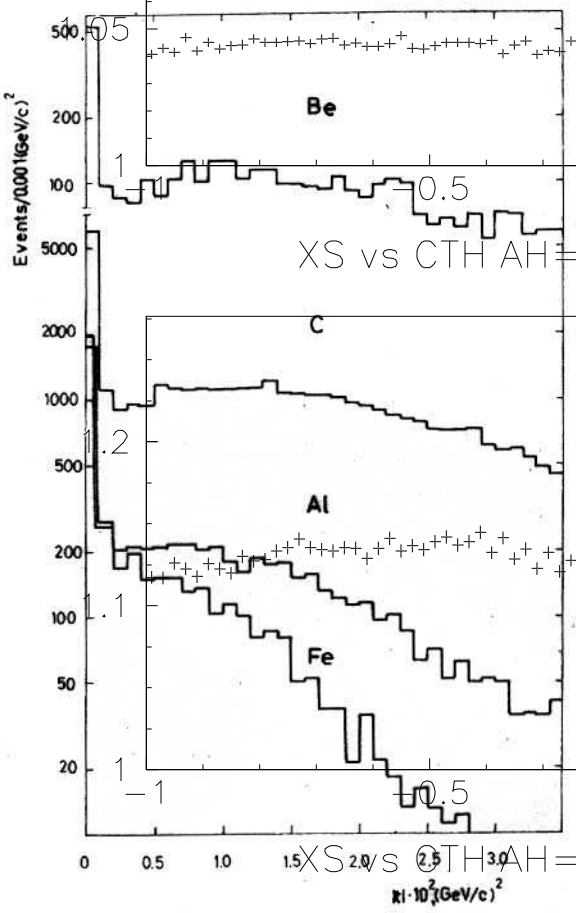

XS vs CTH AH=BH=0 * ephot = 230.− 350.

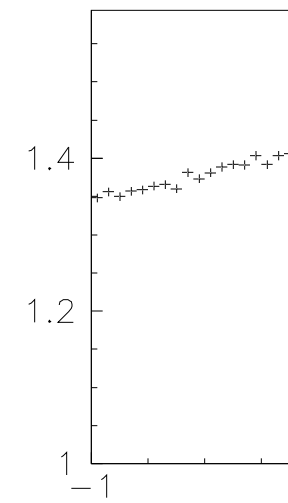

XS

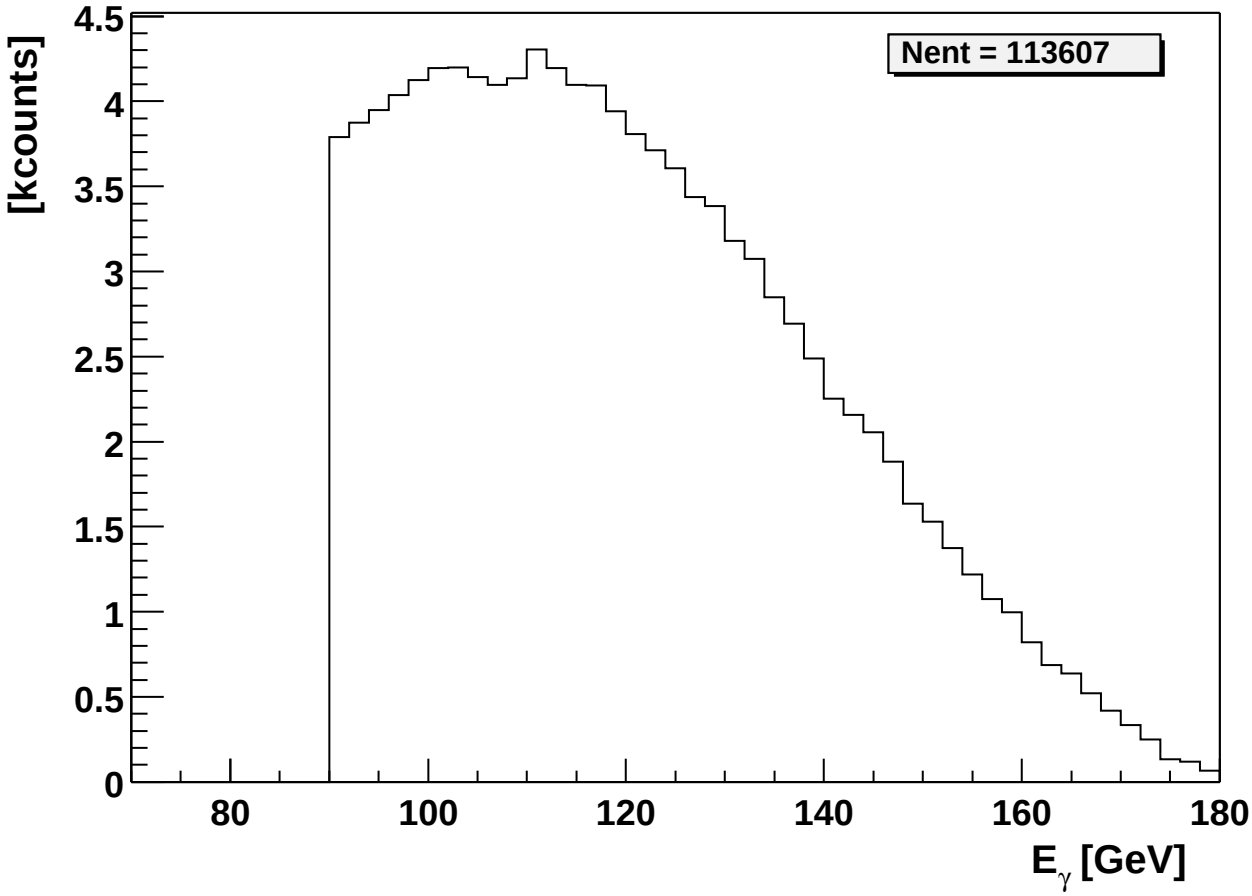
Nent = 113607
[kcounts]
4.5
4
3.5
3
2.5
2
1.5
1
0.5
0
80
100
120
140
160
180
E_γ [GeV]

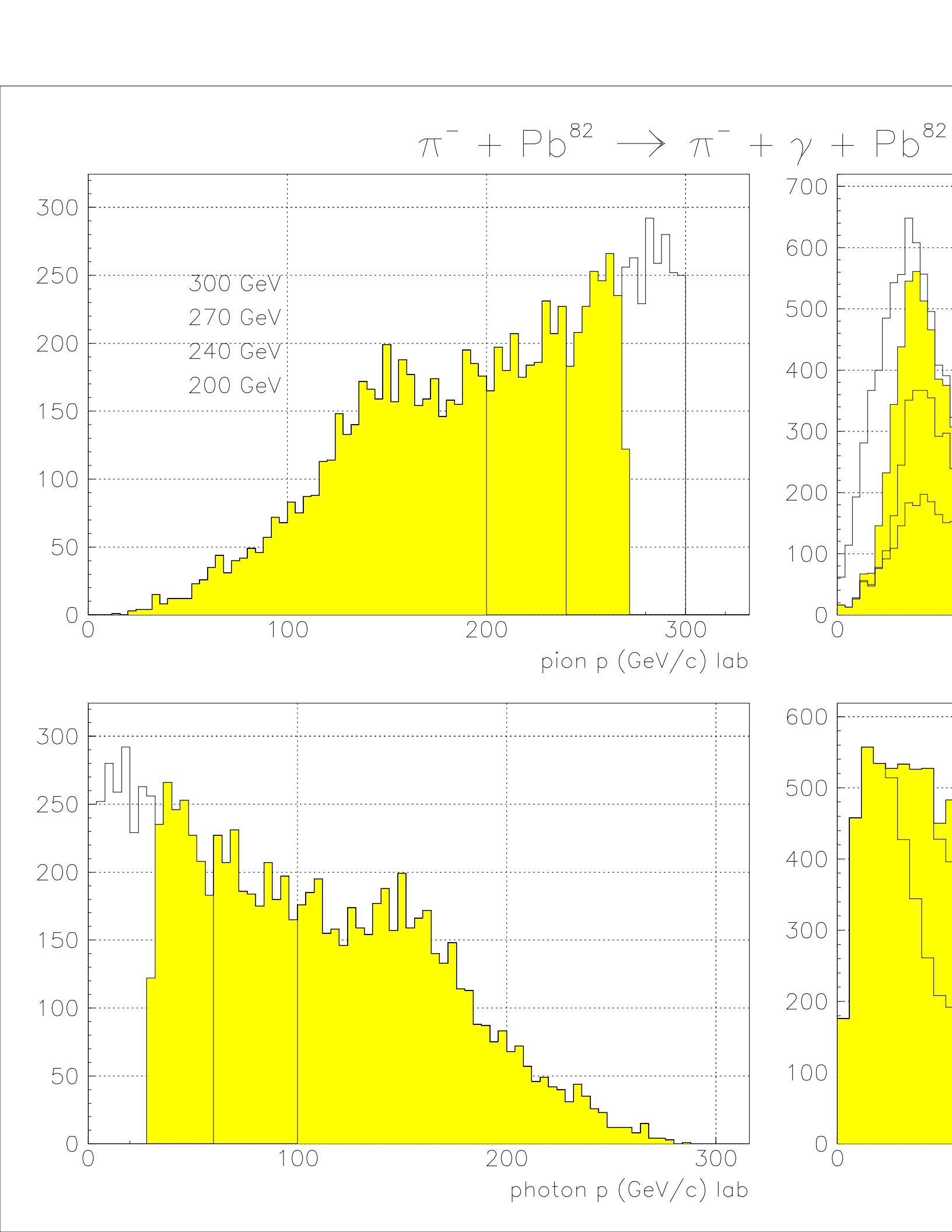
$\pi^- + Pb^{82} \rightarrow \pi^- + \gamma + Pb^{82}$
300 GeV
270 GeV
240 GeV
200 GeV
pion p (GeV/c) lab
photon p (GeV/c) lab

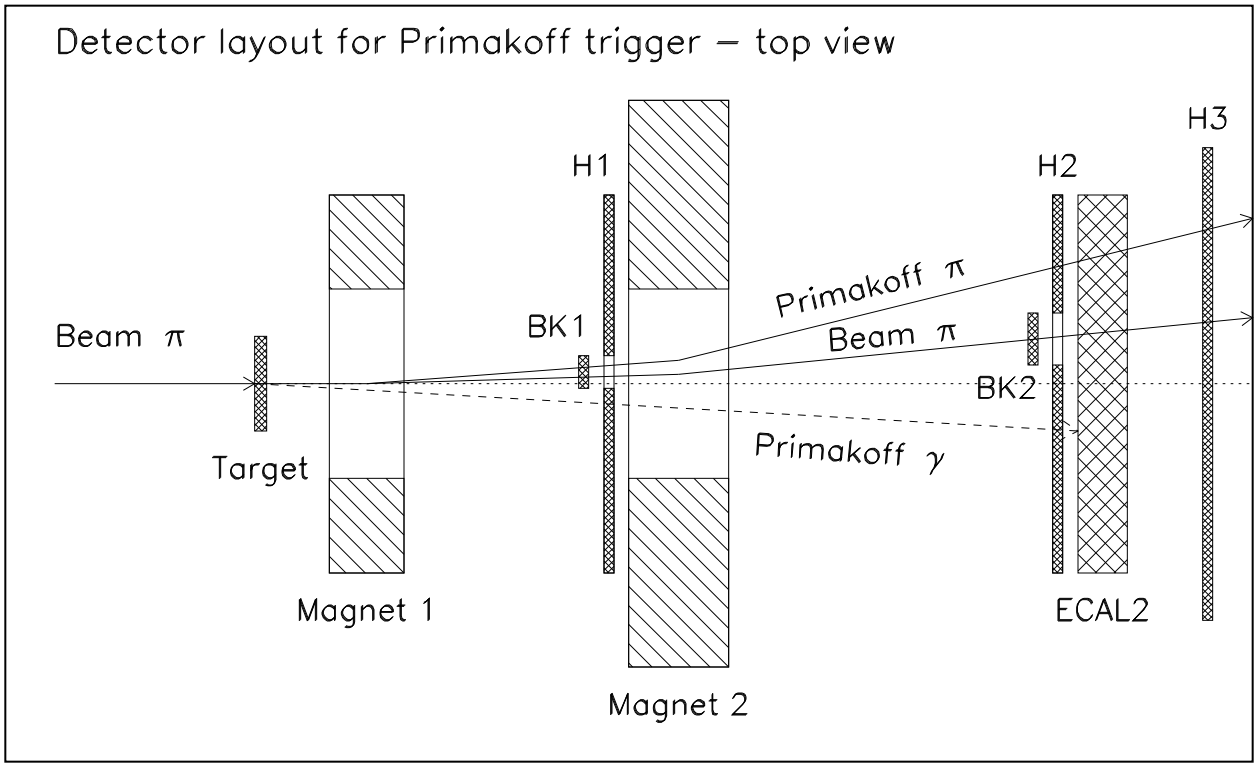
Detector layout for Primakoff trigger – top view
H3
H1
H2
Primakoff π
Beam π
Beam π
BK1
BK2
Primakoff γ
Target
Magnet 1
ECAL2
Magnet 2

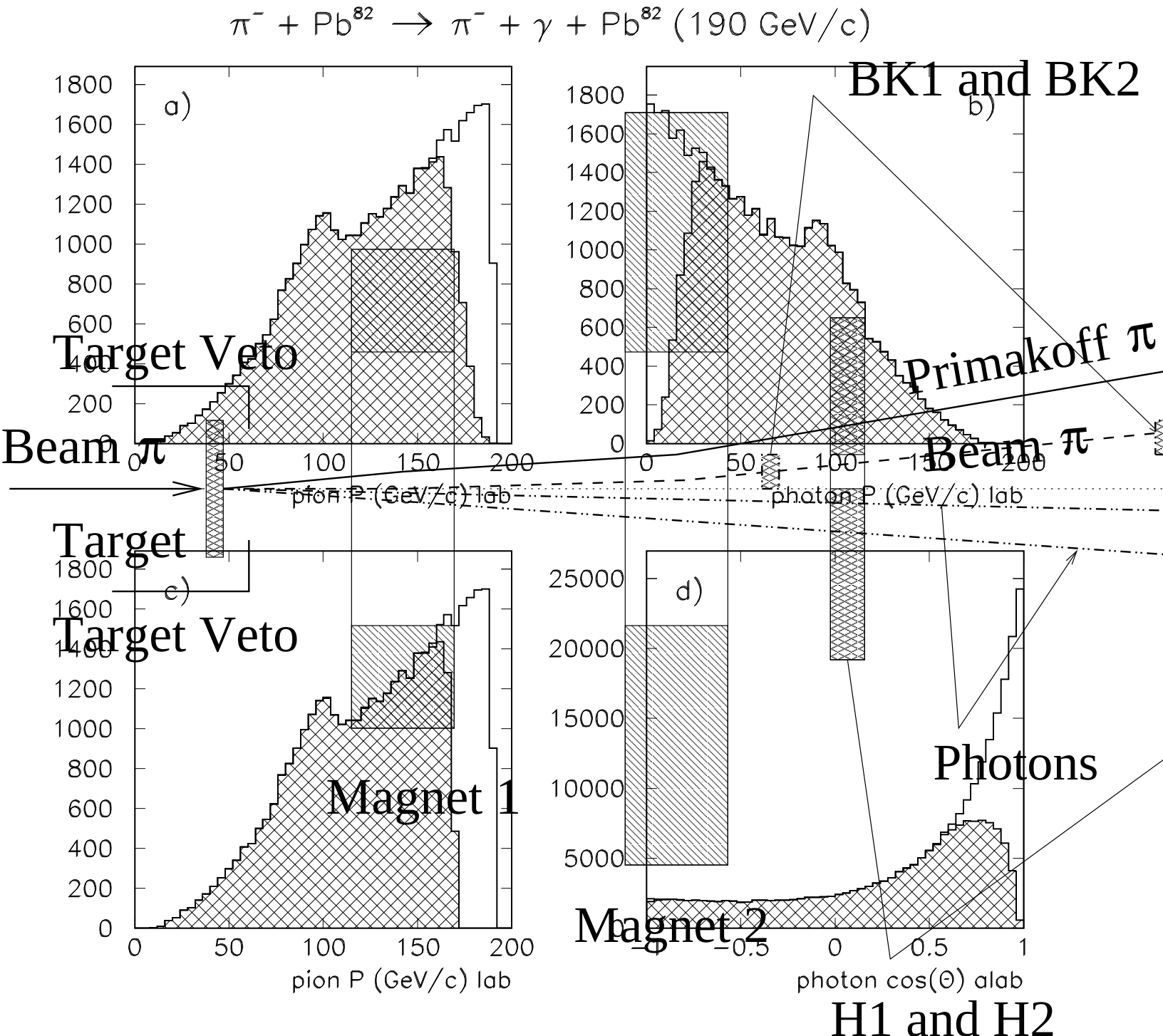
$\pi^- + Pb^{82} \rightarrow \pi^- + \gamma + Pb^{82}$ (190 GeV/c)
a)
b)
c)
d)
pion P (GeV/c) lab
photon P (GeV/c) lab
photon cos(Θ) alab
BK1 and BK2
Target Veto
Primakoff π
Beam π
Beam π
Target
Target Veto
Photons
Magnet 1
Magnet 2
H1 and H2